NASA TECHNICAL NOTE

NASA TN D-4231

NASA TN D-4231

STATIC, SUBSONIC, AND SUPERSONIC OXIDATION OF JT GRAPHITE COMPOSITES

by John D. Buckley

Langley Research Center
Langley Station, Hampton, Va.

NATIONAL AERONAUTICS AND SPACE ADMINISTRATION • WASHINGTON, D. C. • OCTOBER 1967

STATIC, SUBSONIC, AND SUPERSONIC OXIDATION OF JT GRAPHITE COMPOSITES

By John D. Buckley

Langley Research Center
Langley Station, Hampton, Va.

NATIONAL AERONAUTICS AND SPACE ADMINISTRATION

For sale by the Clearinghouse for Federal Scientific and Technical Information
Springfield, Virginia 22151 – CFSTI price $3.00

STATIC, SUBSONIC, AND SUPERSONIC OXIDATION OF JT GRAPHITE COMPOSITES

By John D. Buckley
Langley Research Center

SUMMARY

An experimental investigation was made to characterize and evaluate the high-temperature performance and self-generating protective oxide coating of three JT graphite composites. The effects of preoxidation on the tensile and compressive strength of JT graphite composite specimens tested at room temperature are shown. Static oxidation tests at temperatures up to 1760° K at 1 atmosphere (101 kN/m^2) and at 1925° K at 1×10^{-6} torr (0.1 mN/m^2) were performed to observe coating formation. Tests made in air, nitrogen, and air-nitrogen mixtures in subsonic and supersonic gas streams produced front-face surface temperatures up to 3000° K. A coating study was made with X-ray diffraction to identify the composition of the composites produced under various atmospheres, pressures, and temperatures. A possible mechanism for the coating formation is discussed.

An oxide coating formed on the JTA graphite composite at elevated temperatures in oxidizing atmospheres provides good resistance to further oxidation under static, subsonic, and supersonic oxidizing conditions. Room-temperature tensile and compressive strength tests of preoxidized specimens showed a decrease in strength with increased temperature and/or time.

INTRODUCTION

A continuing need exists for structural materials that can be used in oxidizing atmospheres at temperatures between 1500° K and 3000° K where extended exposure oxidizes coated refractory metals and ablation materials may not be suitable for long time use. Graphite-base refractory composites labeled JT have been developed recently to improve oxidation resistance of graphite. These materials have a density of about 191 lbm/ft^3 (3060 kg/m^3) and relatively good resistance to oxidation at elevated temperatures (ref. 1). The JT graphite composites consist of mixtures made up primarily of graphite and zirconium diboride or zirconium carbide with small additions of silicon and columbium. (See ref. 2.) The resistance to oxidation achieved by these materials is due to thermochemical reactions which generated a self-protective oxide coating.

Recent work has been done to characterize and correlate the physical and mechanical properties of JTA, particularly at elevated temperatures (ref. 3). Limited studies have also been made of the oxidation resistance of JTA under static and dynamic oxidizing conditions (ref. 2).

A study was undertaken at the Langley Research Center to extend the present information on high-temperature oxidation and to characterize the high-temperature performance and self-generating protective coating on JTA and two experimental grades (JT-0981 and JT-0965) of JT graphite composites. (See ref. 2 for specifications of these graphite composites.) The investigation covered the determination of tensile and compressive properties of specimens that had been preheated up to 1760° K, the determination of the effects of static and dynamic oxidation, and X-ray diffraction and metallographic studies to aid in characterizing the coating mechanism.

The units used for the physical quantities in this paper are given both in the U.S. Customary Units and in the International System of Units (SI) (ref. 4). Appendix A presents factors relating these two systems of units.

MATERIALS AND SPECIMENS

The nominal composition of JTA, JT-0981, and JT-0965 (the three composites investigated) is shown in table I. These composites were produced in a one-step hot-pressing operation at temperatures ranging from 2073° K to 3373° K and molding pressures between 2.25 ksi and 6.35 ksi (15.5 and 43.8 N/m^2) depending on the composition (ref. 5). Two lots of materials were supplied by the vendor over a period of 2 years. X-ray analysis of the as-received materials of both lots showed that the composition was the same. Mechanical and oxidation test specimens were machined from cylindrical stock 7.7 cm in diameter by 7.7 cm in length. The configurations of the dynamic oxidation and tensile specimens are shown in figures 1(a) and (b), respectively. The compressive test specimens were cubes 1.27 cm on a side and the static oxidation specimens were small square pieces 1.27 cm on a side by 0.63 cm thick. A diamond-point stylus profilometer indicated that surfaces of machined specimens had a roughness of 0.4μm rms. The tensile and compressive strength test specimens were machined so that testing loads were applied in the across-the-grain or weakest direction (ref. 5).

APPARATUS AND TEST PROCEDURE

Mechanical Properties Tests

Tensile and compressive tests at room temperature were conducted in a 100-kip (445 kN) hydraulic-powered testing machine at a head speed of 0.13 mm per minute until fracture. Grips used in the tensile tests were split-collar assemblies. The spherical button head was continuously supported by a mating surface on the collar. This fixture provided self-alinement for the specimen. Compression specimens with machined parallel surfaces bore directly on the platen surfaces. Maximum load was recorded from the dial of the testing machine.

Oxidation Tests

Static.- Static oxidation tests were conducted in an electrically heated furnace at 1 atmosphere (101 kN/m^2) and 1×10^{-6} torr (0.1 mN/m^2) at 1925° K.

Specimens at ambient pressure in air were suspended by a platinum wire into the precalibrated heat zone of the vertical-tube furnace with a closed bottom. The test time for these specimens varied from 1 to 24 hours over a temperature range from 1365° K to 1760° K. The specimens tested in the vacuum furnace were exposed for the same period of time over a temperature range from 1365° K to 1925° K at a pressure of 1×10^{-5} or 1×10^{-6} torr (1 to 0.1 mN/m^2). All specimens were measured and weighed before and after testing.

Dynamic.- Dynamic oxidation tests were performed in the 2.5-megawatt atmospheric arc jet (fig. 2) described in reference 6 and the 2.5-megawatt supersonic arc tunnel (fig. 3) described in references 7 and 8. The pertinent mechanical and electrical features of both facilities remain unchanged under subsonic or supersonic operating conditions. Supersonic flow was obtained by utilizing supersonic nozzles in the test. In the arc tunnel the flow was exhausted into a vacuum sphere.

For the dynamic oxidation tests two nozzle shapes were used to produce the subsonic and supersonic flow conditions. Test conditions are shown in table II. The heating rates were measured with a metal calorimeter having the same dimensions and shape as the specimen shown in figure 1(a). The gas temperature at the nozzle was calculated by using the sonic method described in reference 6 for subsonic conditions and in reference 9 for supersonic conditions. The surface temperature of the heated specimens was measured with an optical pyrometer using an emittance value for zirconia of 0.8 (ref. 10).

The subsonic test specimens were mounted in the 2.5-MW atmospheric arc jet (fig. 2) on a 2.2-cm-diameter water-cooled sting so that the front surface of the specimen was 4.3 cm above the arc jet nozzle which exited into the air (condition A, table II). Each graphite composite specimen was exposed for 3 to 10 cycles of 6-minute duration. After each 6-minute exposure the specimen was removed and measured to determine surface recession.

The supersonic test specimens were placed in either the 2.5-MW arc jet (fig. 2) (condition A, table II) or the 2.5-MW supersonic arc tunnel (fig. 3). The specimens subjected to condition C, table II, were tested in the 2.5-MW atmospheric arc jet under conditions similar to those for the subsonic test specimens except that the composition of the gas stream and the duration of exposure cycle were varied and pressure times ranged from 40 to 80 seconds per cycle in air and in the mixture of 10 percent oxygen and 90 percent nitrogen. Each exposure cycle in nitrogen lasted 40 seconds. Exposure time was limited by facility capability.

The specimens tested in the supersonic arc tunnel were mounted on a water-cooled sting about 3 cm downstream from the arc jet nozzle. The specimen was inserted into the test section for exposures of 2 minutes. The gases used were of the same composition as those used in the preceding tests. The exposure time was again limited by facility capability.

Metallurgical Studies

X-ray diffraction analyses and optical macrostructure examinations were made of the coatings produced on specimens in the static and dynamic oxidation tests to obtain an understanding of the mechanism of coating formation. X-ray diffraction patterns were made of the various coated surfaces and of coatings removed and reduced to -325 mesh powder by grinding. Specimens were placed in the XRD-6 diffractometer and scanned by using a collimated copper K alpha X-ray beam with a nickel filter. A scanning angle between 15° and 65° was used and the diffraction pattern was recorded on a strip chart recorder. The patterns were indexed and the materials were identified by comparing them with information in the American Society of Testing Materials card data file. Metallographic examinations were made of the surfaces of the tested oxidation specimens. Photographs at magnifications varying from 2 diameters to 4 diameters were made to show the appearance of the coated surfaces of the test specimens.

RESULTS AND DISCUSSION

Mechanical Properties

Tensile tests.- The results of the room-temperature tensile tests on the JTA graphite composite are presented in figure 4. The as-received tensile specimens show a strength of about 6 ksi (41 MN/m^2). After 4 hours of exposure in a closed-bottom vertical-tube furnace at 1365° K and 1760° K, the tensile strength was 50 and 25 percent of the unexposed strength, respectively. Exposure up to 24 hours at these temperatures had little additional effect on the tensile strength. These changes in strength probably resulted from structural changes in the test specimens due to the thermochemical reactions produced when JTA composite material is subjected to oxidizing atmospheres at elevated temperatures.

Compression tests.- The compression tests on JTA composite material showed little change in strength after a 24-hour exposure at 1365° K but a gradual loss in strength at 1760° K during the 24-hour exposure (fig. 5). The rather small change in compressive strength at 1365° K contrasted to the large change in tensile strength at the same temperature (fig. 4) is attributed to the basic characteristic of ceramic materials to carry greater loads in compression than in tension at relatively low temperatures. The compressive strength at 1760° K, however, decreased about 50 percent after 16 hours of exposure.

Static Oxidation

Tests in air.- The results of the static oxidation tests on the JT graphite composites subjected to elevated temperatures in the vertical-tube furnace are presented in figures 6, 7, and 8. These tests were made at 1365° K and 1760° K at exposure times ranging from 1 to 24 hours. Figures 6(a) and (b) show the mass loss percent of material due to oxidation for the three graphite composites tested. The JTA specimens exposed at each temperature had a mass loss of no more than 12 percent, whereas the mass loss of the other composites at either test temperature was never less than 18 percent and was as high as 34 percent. Also, a comparison of figures 6(a) and (b) indicates that the JT-0981 and JT-0965 specimens had a decrease in mass loss with increasing temperature rather than the expected increase of the JTA specimen. This decrease in mass loss at the higher temperature is probably due to the increased protection afforded the specimen by the coatings (figs. 7 and 8) which formed more effectively at the higher temperatures. The coating mechanism, discussed subsequently in this paper, can be described as a thermochemical reaction between oxygen and the other components or compounds in the graphite composite.

Photographs of specimens tested at 1365° K in air are presented in figure 7 for exposure times of 0, 4, 8, and 24 hours. The JTA composite specimens have a glass-like coating on the surfaces, whereas the JT-0965 and JT-0981 specimens have no coating and show general deterioration. Destructive oxidation of zirconium carbide (a major component of JT-0965 and JT-0981), characterized by Kuriakose and Margrave (ref. 11), is believed to be the cause of deterioration of these JT graphite specimens.

All specimens subjected to oxidizing conditions at 1760° K survived for 24 hours (fig. 8). Examination of the specimens indicates that the amount of coating formed on all the JT composites, particularly JTA, increased with time at this high temperature. It is believed that the thickness of the glass-like coating produced on the specimens exposed to 1760° K is the factor that provided protection. The initial reaction between the oxidizing atmosphere and the specimen surface at high temperature produced oxidation before a protective coating developed; this caused distortion of the JT-0981 specimens within the first hour of testing. No further degradation of the specimens was observed for any longer test time.

Tests in vacuum.- To determine whether oxygen was the impetus for producing a coating on JT graphite composites, static oxidation tests were made at 1365° K and 1925° K and at pressures ranging from 1×10^{-5} to 1×10^{-6} torr. Examination of specimens showed no significant change in weight. The tests indicated that these graphite composite materials were unaffected by heating up to 1925° K at reduced pressures and that the formation of the protective coatings on JT graphites required oxygen in the environment. The nature of the coating formed depended on the surface temperature of the specimen.

Dynamic Oxidation

Subsonic airflow tests.- Arc jet tests under subsonic airflow conditions (condition A, table II) were made on JTA, JT-0965, and JT-0981 graphie composites to observe the effects of subsonic airflow on oxidation and erosion resistance at elevated temperatures. Table III gives subsonic test data for total recession along the longitudinal axis of the specimens as a function of the accumulated cyclic exposure time. The tests of the JTA composite were concluded after a total accumulated exposure time of 1 hour. The greater mass loss rate for the other composites necessitated the conclusion of tests of these materials after shorter periods of time. Note in table III that the JTA composite has greater resistance to oxidation than the other materials when subjected to subsonic airflow which produces a front-face surface temperature of 2475° K.

Photographs of the specimens subjected to subsonic airflow show that the JTA composite (fig. 9(a)) maintained a relatively uniform shape during testing and that a white protective coating covered most of the specimen after ten 6-minute exposures. The photographs of the JT-0981 and JT-0965 specimens (fig. 9(b) and fig. 9(c), respectively) show that, although the hot front surfaces of these specimens maintained their shape or symmetry, the cylindrical portions of the specimens eroded unevenly. Visual examination of the JT-0965 and JT-0981 specimens indicated that material loss due to high-temperature subsonic airflow was less on the hot face surfaces where coatings were present than on the uncoated or sparsely coated cylindrical surfaces. The relatively uniform protective coating formed on all surfaces of the JTA composite and the lack of a uniform coating on the JT-0965 and JT-0981 composites indicated that the coating inhibits oxidation of the graphite composites.

One characteristic observed in tests of the JT composites, particularly the JTA, was the resistance to cracking under rapid temperature changes. Examination of all specimens showed no cracks after four or more 6-minute cycles. The specimens were thrust from room temperature into the 3650° K arc jet stream and reached 95 percent of the front-face surface test temperature of 2475° K within 20 seconds. It is believed that the relatively high thermal conductivity of the composites was an important factor in the resistance of this material to cracking under nonuniform or rapidly varying temperatures.

Supersonic flow tests.- The good high-temperature performance of JTA in the subsonic airflow tests led to further investigation of this composite under supersonic flow conditions. The results of tests of specimens in supersonic gas flow (condition B, table II) at surface temperatures of 2500° K are shown in table IV. Comparison of the recession of JTA in subsonic airflow at a specimen surface temperature of 2475° K with the recession of JTA in supersonic gas flow at approximately the same temperature indicated that total recession was more severe under supersonic conditions (fig. 10).

The calculated total recession of ATJ graphite under the same supersonic test conditions (condition B, table II) is also presented in figure 10. This recession was determined by dividing the total mass loss obtained from equation (B5) of reference 12 by the density of ATJ (108 lbm/ft^3 or 1730 kg/m^3). Total recession was calculated for a 1-minute exposure. Comparison of the recession data for JTA and ATJ graphite composites in figure 10 indicates that the total recession of ATJ for short periods of time is much greater than that for JTA.

To determine whether recession obtained in the supersonic flow tests was largely due to oxidation, tests were performed at a constant specimen surface temperature of 2500° K and approximately the same stagnation pressure in air and modified atmospheres containing nitrogen and a mixture of 10 percent oxygen and 90 percent nitrogen (table II). Data in table IV and figure 11 show that little or no recession took place on specimens exposed to nitrogen and that surface recession and magnitude of the coating formed increased with addition of oxygen to the gas stream. These data indicate that the thermochemical reaction of oxygen in the 2500° K gas stream coupled with the effect of increased pressure gradient across the front surface of the specimen produced the observed recession.

Supersonic tests were also made with the 2.5-MW atmospheric arc jet operating at maximum capability to observe the effect of severe thermal and gas flow conditions on JTA specimens (condition C, table II). Data in table V and figure 12 show negligible recession or coating formation on specimens subjected to nitrogen gas flow; surface recession and coating formation increased with increasing oxygen content in the gas stream of the arc jet. These results indicate that under these conditions (air at about 3000° K) oxygen and front-face surface temperature were responsible for activating the thermochemical process necessary to produce the molten oxide coatings and subsequent recession on JTA graphite composite. This result was substantiated by the fact that the more severe nitrogen gas stream temperatures of 4800° K and stagnation pressures of 4 atmospheres produced negligible recession on the JTA specimens.

Coating Studies

X-ray investigation.- X-ray diffraction techniques were used to study the composition of JTA graphite composite as received and after static and dynamic oxidation tests. The results of the X-ray diffraction measurements are presented in tables VI and VII and figures 13 and 14. The d-spacing calculated from the diffraction record for the as-received JTA graphite composite (table VI) agrees with the d-spacing for carbon, zirconium diboride, and silicon carbide from the ASTM X-ray cards. This information indicates that zirconium diboride, silicon carbide, and graphite existed in the as-received composite. Table VII gives the d-spacing for the compounds which are formed after exposure at 2475° K in a dynamic airstream and identified as the oxide of zirconium and zirconium silicate by a comparison with the values from the ASTM cards. The appearance of these new surface compounds indicates that thermochemical reactions did take place in the presence of air at elevated temperatures (ref. 11). X-ray patterns in figure 13 graphically depict peaks due to exposure of JTA to elevated temperatures under dynamic airflow conditions. Of particular significance was the absence in the coating material of all the peaks representing the original composition. Zirconia, zirconium silicate, and amorphous silica were the components of the coating produced from the exposure of JTA in still air for 24 hours at 1365° K (table VII and fig. 14(a)). The progressive broadening of the peaks at a higher temperature of 1760° K observed in the X-ray patterns in figure 14(b) is indicative of the effect of the amorphous component of the coating. The zirconium silicate peaks in the 1365° K pattern disappeared in the 1760° K pattern; this suggests that a series of thermochemical reactions took place before the zirconia coating formed.

Coating mechanism.- Data obtained from the X-ray analysis of the protective oxide coating formed on JTA graphite specimens suggested a probable explanation of the coating mechanism. This mechanism is based on reactions of each of the components that make up JTA composite with oxygen and/or the products of oxidation. The initial reactions are as follows:

Carbon + Oxygen → Carbon monoxide
(1) $2C + O_2 \longrightarrow 2CO\ (g)\uparrow$ (ref. 13)

Carbon dioxide
(2) $C + O_2 \longrightarrow CO_2\ (g)\uparrow$ (ref. 13)

Silicon carbide + Oxygen → Silica + Carbon monoxide
(3) $2SiC + 3O_2 \longrightarrow 2SiO_2\ (\ell) + 2CO\ (g)\uparrow$ (ref. 14)

Zirconium diboride + Oxygen → Zirconia + Boric oxide
(4) $2ZrB_2 + 5O_2 \longrightarrow 2ZrO_2\ (s) + 2B_2O_3\ (\ell)$ (ref. 11)

Zirconia-Silica → Zirconium silicate
(5) $ZrO_2 + SiO_2 \longrightarrow ZrSiO_4$ (ref. 15)

where

(s) solid
(l) liquid
(g) gas

The molten boron oxide produced in reaction (4) has a melting point of 723° K (ref. 16, fig. 207). This molten oxide forms a protective layer on the specimen surface and subsequently slowly vaporizes at approximately 1530° K (ref. 11). Silicon carbide also reacts with oxygen to produce amorphous silica at temperatures as low as 1175° K (ref. 14). This amorphous silica protects the JTA specimen up to temperatures of 1905° K where it is noticeably dissipated into the vapor state (ref. 17).

A product of an intermediate reaction between zirconia and silica is zirconium silicate (ref. 15) observed in the X-ray pattern in figure 14(a). It is believed that this compound decomposes at approximately 1760° K (ref. 15). The zirconia produced by this decomposition reacts with silica and other additives in the composite as the specimen recesses to produce the molten zirconia coating, which protects the specimens subjected to supersonic airstreams up to a surface temperature of 2975° K.

Macrostructure.- Metallographic examination of the coatings formed on the JTA graphite composite under dynamic oxidizing conditions showed a pitted front-face coating on the subsonic test specimen (fig 15(a)) and a smooth coating on the supersonic test specimen (fig. 15(b)). The reason for the different appearance was deduced from an examination of static oxidation specimens (fig. 16) heated at 1760° K at 8 and 24 hours and from micrographs of coating cross sections of the front surface of the subsonic and supersonic specimens (fig. 17). The pitted surfaces observed on the static and dynamic specimens are believed to have been caused by several chemical reactions at the interface of the oxide coating and the virgin material. These reactions taken from reference 18 are as follows:

(A) $SiO_2 + 3C \rightarrow SiC + 2CO$

(B) $ZrSiO_4 + 6C \rightarrow ZrC + SiC + 4CO$

(C) $2B_2O_3 + 7C \rightarrow B_4C + 6CO$

(D) $ZrO_2 + 3C \rightarrow ZrC + 2CO$

All the oxides that make up the coating reacted with virgin graphite at the interface of the coating and the virgin material to produce various carbides and carbon monoxide which can escape in the form of bubbles. In view of the molten state of the coating, the ambient pressure during the static oxidation exposure, and the fact that the pressure in the subsonic and supersonic airstreams was less than the equilibrium pressure of the carbon monoxide (fig. 18), it appears that carbon monoxide produced at the interface of the coating and the virgin material moved to the surface of the molten coating and caused bubbles and pits (fig. 17(a)). The absence of a macroscopic pitted surface on specimens tested in the supersonic airstream (fig. 17(b)) is believed to be due to the thinner coating formed under supersonic flow conditions (condition B, table II). With the thin coating the gas bubbles were unable to coalesce into larger bubbles which formed the macroscopic pits on the surface of the subsonic test specimens.

SUMMARY OF RESULTS

A study was made to characterize the protective coating on JT graphite composites and to determine its influence on material strength and structure. The results of the study are as follows:

1. The coating which forms on the JTA composite appears to be the major factor in providing relatively good oxidation resistance in supersonic airstreams up to 3000° K. The coating is produced from a series of thermochemical reactions between the original components of the composite and oxygen.

2. The calculated surface recession of ATJ graphite is much greater than the recession of JTA composite in a supersonic airstream for short periods of time. It appears that oxygen is the gaseous component of the supersonic airstream which produces the molten protective oxide coating on JTA.

3. Minimal surface recession was noted on JTA specimens subjected to supersonic nitrogen gas streams of 4800° K under conditions similar to the supersonic airstream tests at temperatures of about 3000° K.

4. The JTA composite exhibited greater resistance to static oxidation than either the JT-0965 or JT-0981 composite at elevated temperatures of 1365° K and 1760° K at 1 atmosphere (101 kN/m^2). None of the JT graphite composites tested were affected under static conditions by elevated temperatures up to 1925° K at reduced air pressure of 1×10^{-5} torr (1 mN/m^2).

5. Room temperature tensile and compressive strengths of JTA graphite composite preoxidized from 4 to 24 hours at 1365° K and 1760° K were reduced by the exposure. The tensile property showed the largest strength decrease percentagewise.

Langley Research Center,
National Aeronautics and Space Administration,
Langley Station, Hampton, Va., April 10, 1967,
129-03-04-01-23.

APPENDIX A

CONVERSION OF U.S. CUSTOMARY UNITS TO SI UNITS

The International System of Units (SI) was adopted by the Eleventh General Conference on Weights and Measures, Paris, October 1960, in Resolution No. 12 (ref. 4). Conversion factors for the units used herein are given in the following table:

Physical quantity	U.S. Customary Unit	Conversion factor (*)	SI Unit
Density.	lbm/ft^3	16.02	kg/m^3
Enthalpy	Btu/lbm	2.32×10^3	J/kg
Heat-transfer rate . .	Btu/ft^2-sec	1.135×10^4	W/m^2
Length	ft	0.3048	m
	in.	0.0254	m
Mass	lbm	0.4536	kg
Flow rate	lbm/sec	0.453592	kg/s
Pressure	torr	133.322	N/m^2
	atm	1.01325×10^5	N/m^2
	ksi	6.89×10^6	N/m^2
Temperature	^{o}F	$\frac{5}{9}(^{o}F + 460)$	^{o}K
Velocity	ft/sec	0.3048	m/s
Stress	ksi	6.89×10^6	N/m^2
Force	kip	4.44822×10^3	N

*Multiply value given in U.S. Customary Unit by conversion factor to obtain equivalent value in SI Unit.

Prefixes to indicate multiples of units are as follows:

Prefix	Multiple
mega (M)	10^6
kilo (k)	10^3
centi (c)	10^{-2}
milli (m)	10^{-3}

REFERENCES

1. Buckley, John D.; and Stein, Bland A.: Preliminary Investigation of the Dynamic Oxidation of JT Graphite Composites at Surface Temperatures Between 4000° F and 5000° F. Summary of the Eleventh Refractory Composites Working Group Meeting, Darrell R. James and Elvin H. Beardslee, [compilers], AFML-TR-66-179, U.S. Air Force, July 1966, pp. 595-614.
2. Carbon Prod. Div., Union Carbide Corp.: Improved Graphite Materials for High-Temperature Aerospace Use. Volume II – Development of Graphite-Refractory Composites. ML-TDR-64-125, Vol. II, U.S. Air Force, Aug. 1964.
3. Bortz, S. A.; and Connors, C. L.: Physical Properties of Refractory Materials. Quart. Rept. No. 6 (Contract No. AF 33(615)-3028), IIT Res. Inst., Dec. 14, 1966.
4. Mechtly, E. A.: The International System of Units – Physical Constants and Conversion Factors. NASA SP-7012, 1964.
5. Zeitsch, K. J.; and Criscione, J. M.: Research and Development on Advanced Graphite Materials. Volume XXX. Oxidation Resistant Graphite Base Composites. WADD TR 61-72, Vol. XXX, U.S. Air Force, Aug. 1963. (Available from DDC as AD 600 340.)
6. Brown, Ronald D.; and Fowler, Bruce: Enthalpy Calculated From Pressure and Flow-Rate Measurements in High-Temperature Subsonic Streams. NASA TN D-3013, 1965.
7. Brown, Ronald D.; and Levin, L. Ross: A 6-Inch Subsonic High-Temperature Arc Tunnel for Structures and Material Tests. NASA TN D-1621, 1963.
8. Brown, Ronald D.: A Comparison of the Theoretical and Experimental Stagnation-Point Heat Transfer in an Arc-Heated Subsonic Stream. NASA TN D-1927, 1964.
9. Jorgensen, Leland H.: The Total Enthalpy of a One-Dimensional Nozzle Flow With Various Gases. NASA TN D-2233, 1964.
10. Wilson, R. Gale: Hemispherical Spectral Emittance of Ablation Chars, Carbon, and Zirconia to 3700° K. NASA TN D-2704, 1965.
11. Kuriakose, A. K.; and Margrave, J. L.: The Oxidation Kinetics of Zirconium Diboride and Zirconium Carbide at High Temperatures. J. Electrochem. Soc., vol III, no. 7, July 1964, pp. 827-831.
12. Miller, Irvin M.; and Sutton, Kenneth: Experimental Study of the Oxidation of Graphite in High-Temperature Supersonic and Hypersonic Environments. NASA TN D-3444, 1966.

13. Campbell, I. E., ed.: High-Temperature Technology. John Wiley & Sons, Inc., c.1956, p. 110.

14. Jorgensen, Paul J.; Wadsworth, Milton E.; and Cutler, Ivan B.: Oxidation of Silicon Carbide. J. Am. Ceram. Soc., vol. 42, no. 12, Dec. 1959, pp. 613-616.

15. Curtis, C. E.; and Sowman, H. G.: Investigation of the Thermal Dissociation, Reassociation, and Synthesis of Zircon. I. Dissociation of Zircon. J. Am. Ceram. Soc., vol. 36, no. 6, June 1953, pp. 190-193.

16. Levin, Ernest M.; Robbins, Carl R.; and McMurdie, Howard F.: Phase Diagrams for Ceramists. The Am. Ceram. Soc., c.1964.

17. Berkowitz-Mattuck, Joan B.; and Kaufman, L. P.: The Influence of Vaporization Processes on Oxidation. Summary of the Tenth Refractory Composites Working Group Meeting, L. N. Hjelm, Darrell R. James, Elvin H. Beardslee, [compilers], AFML-TR-65-207, U.S. Air Force, Aug. 1965, pp. 251-268.

18. Zeitsch, Karl J.: Development of Graphite-Base Refractory Composites With Oxidation Resistance at Very High Temperatures. Summary of the Eighth Refractory Composites Working Group Meeting – Volume III, Darrell R. James and L. N. Hjelm, [compilers], ML-TDR-64-233, U.S. Air Force, Jan. 1964, pp. 924-936.

TABLE I.- NOMINAL COMPOSITIONS AND DENSITY OF JT GRAPHITE COMPOSITES

Graphite composite	Analysis, percent by weight					Bulk density	
	C	Zr	Si	B	Cb	lbm/ft^3	kg/m^3
JTA	48	35	9	8	0	190	3040
JT-0965	48	43	7	0	2	190	3040
JT-0981	48	35	17	0	0	192	3075

TABLE II.- SUBSONIC AND SUPERSONIC OXIDATION TEST CONDITIONS

	Test condition A	Test condition B			Test condition C		
	2.5-MW atm arc jet	2.5-MW supersonic arc tunnel			2.5-MW atm arc jet		
	Subsonic flow	Supersonic flow (low temperature)			Supersonic flow (high temperature)		
	Air	Air	10% O_2 90% N_2 (volume)	100% N_2 (volume)	Air	10% O_2 90% N_2 (volume)	100% N_2 (volume)
(a) SI Units							
Nozzle exit, cm	5.1	5.1	5.1	5.1	4.5	4.5	4.5
Nozzle throat, cm	5.1	3.8	3.8	3.8	3.8	3.8	3.8
Gas flow, kg/s	0.16	0.20	0.20	0.20	0.32	0.32	0.32
Arc power, kW	2000	2850	3050	3100	3600	3600	3600
Velocity, m/s	880	1890	1960	1990	1825	1870	1925
Mach number	0.75	2	2	2	1.8	1.8	1.8
Total stream temperature, ^{o}K	3650	3400	3750	4500	3800	4000	4800
Specimen surface temperature, ^{o}K	2475	2500	2500	2500	2975	2865	2755
Enthalpy, MJ/kg	6.5	5.1	5.7	5.7	6.1	6.1	6.1
Heating rate to 3.17-cm-diameter round face (fig. 1), MW/m^2	4.0	5.2	5.6	5.6	6.9	6.9	6.9
Model stagnation pressure, N/m^2 × 10^5	1.42	2.02	2.23	2.33	3.74	3.79	4.04
(b) U.S. Customary Units							
Nozzle exit, in.	2	2	2	2	1.75	1.75	1.75
Nozzle throat, in.	2	1.5	1.5	1.5	1.5	1.5	1.5
Gas flow, lbm/sec	0.35	0.45	0.45	0.45	0.7	0.7	0.7
Arc power, kW	2000	2850	3050	3100	3600	3600	3600
Velocity, ft/sec	2890	6230	6440	6530	6000	6165	6330
Mach number	0.75	2	2	2	1.8	1.8	1.8
Total stream temperature, ^{o}F	6100	5700	6300	7600	6400	6700	8200
Specimen surface temperature, ^{o}F	4000	4000	4000	4000	4900	4700	4500
Enthalpy, Btu/lbm	2700	2200	2450	2450	2650	2650	2650
Heating rate to $1\frac{1}{4}$-in-diameter round face (fig. 1), Btu/ft^2-sec	350	460	500	500	610	610	610
Model stagnation pressure, atm	1.41	2	2.2	2.3	3.7	3.75	4

TABLE III.- RECESSION OF JT GRAPHITE COMPOSITES AT SURFACE TEMPERATURE OF 2475° K IN SUBSONIC AIRFLOW IN 2.5-MW ATMOSPHERIC ARC JET

Accumulated cyclic exposure time, min	Total recession, cm[1]		
	JTA	JT-0981	JT-0965
6	0.025	0.076	0.051
12	.051	.076	.102
18	.127	.280	[2].483
24	.152	.483	
30	.152	[2].637	
36	.250		
42	.280		
48	.371		
54	.432		
60	.457		

[1] Each measurement is an average of three tests.

[2] Test stopped because of extensive loss of material.

TABLE IV.- RECESSION OF JTA GRAPHITE COMPOSITE AT SURFACE TEMPERATURE OF 2500° K IN SUPERSONIC GAS FLOW IN 2.5-MW SUPERSONIC ARC TUNNEL

Accumulated cyclic exposure time, min	Total recession, cm[1]		
	Air	90% N_2 10% O_2	100% N_2
2	0.204	0.127	0
4	.371	.280	.025

[1] Each measurement is an average of three tests.

TABLE V.- RECESSION OF JTA GRAPHITE COMPOSITE AT ELEVATED TEMPERATURE IN SUPERSONIC GAS FLOW IN 2.5-MW ATMOSPHERIC ARC JET

Accumulated cyclic exposure time, min	Total recession, cm[1]		
	Air at 2976° K	90% N_2 and 10% O_2 at 2865° K	100% N_2 at 2755° K
0			
.66	0.076	0.102	0.025
1.33	.371		.051
2.00		.250	.076
2.66	.965		.127
3.33		.371	.152
4.00	1.660	.406	.204

[1] Each measurement is an average of three tests.

TABLE VI.- MAJOR X-RAY DIFFRACTION PEAKS FOR AS-RECEIVED JTA GRAPHITE COMPOSITE

Scanning angle, 2θ,* deg	*d-spacing, Å	d-spacing for carbon from ASTM card, Å	d-spacing for zirconium diboride from ASTM card, Å	d-spacing for β silicon carbide from ASTM card, Å	Reflecting plane
25.20	3.53		3.53		001
26.50	3.36	3.32			002
32.60	2.74		2.74		100
35.70	2.51			2.51	111
41.70	2.16		2.16		101
54.60	1.68	1.63			004
60.00	1.54			1.54	220
71.80	1.31			1.31	311

*From Braggs law

$$n\lambda = 2d \sin \theta$$

where

λ X-ray wavelength

d distance between successive parallel lattice planes

θ one-half the scanning angle

n assumed to be 1

TABLE VII. - MAJOR X-RAY DIFFRACTION PEAKS FOR OXIDIZED JTA GRAPHITE COMPOSITE

Scanning angle, 2θ,* deg	*d-spacing, Å	d-spacing for zirconium oxide from ASTM card, Å	d-spacing for zirconium silicate from ASTM card, Å	Reflecting plane
27.00	3.30		3.30	200
28.22	3.16	3.16		111
31.48	2.84	2.84		111
34.18	2.62	2.62		002
34.46	2.60	2.60		020
35.32	2.54	2.54		200
35.62	2.52		2.52	112
43.78	2.07		2.06	301

*From Braggs law

$$n\lambda = 2d \sin \theta$$

where

λ X-ray wavelength

d distance between successive parallel lattice planes

θ one-half the scanning angle

n assumed to be 1

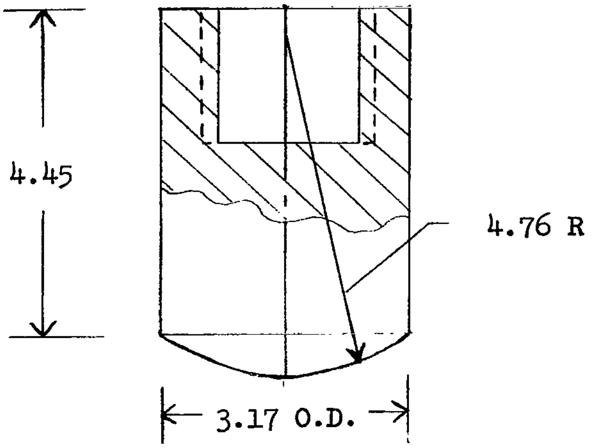

(a) Dynamic oxidation specimen.

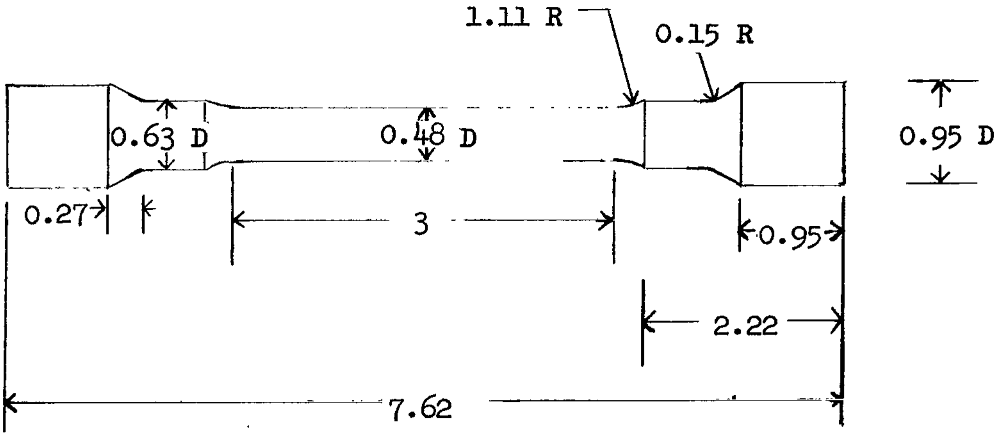

(b) Tensile specimen.

Figure 1.- Specimens of JT graphite composite. All dimensions are in centimeters.

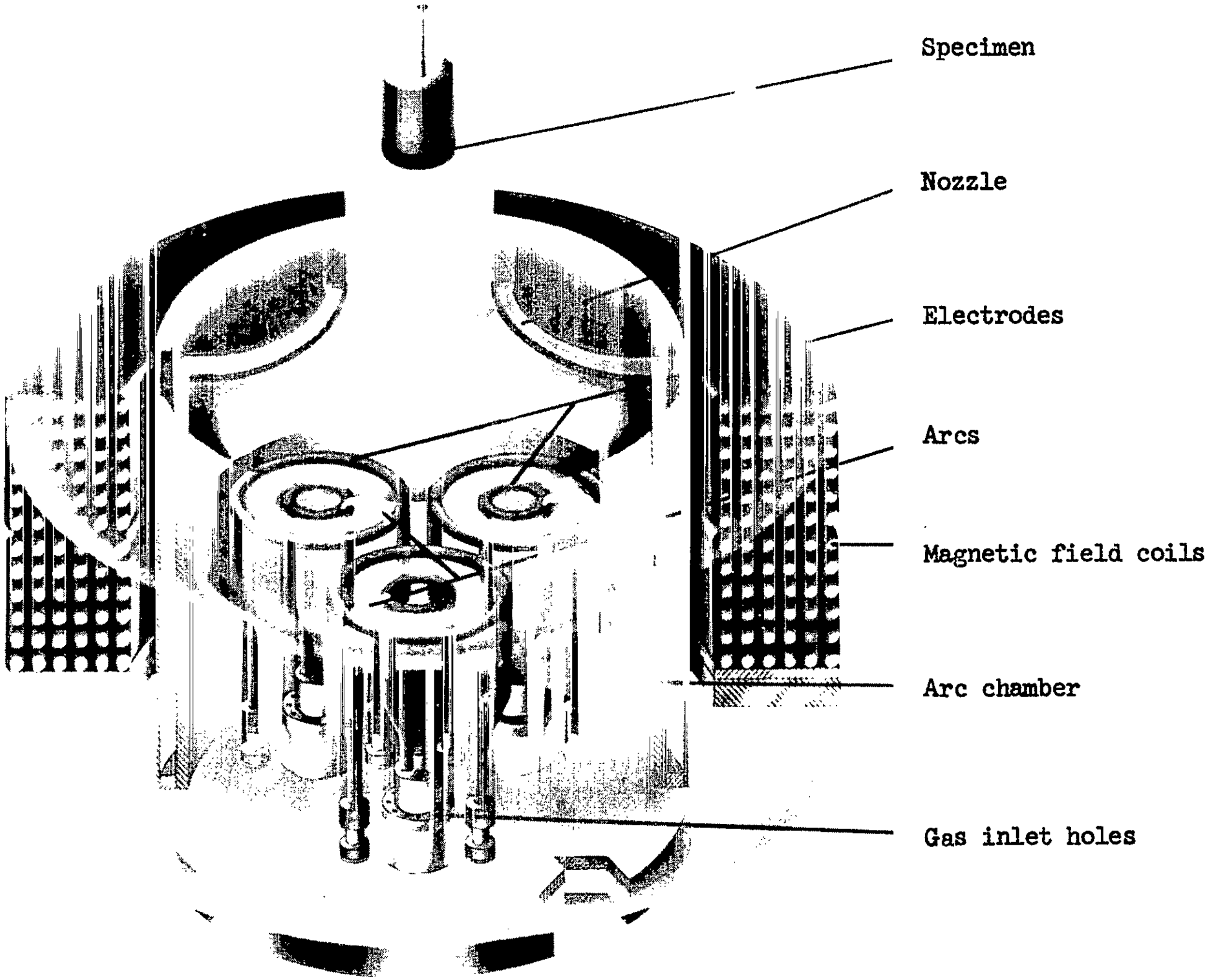

Figure 2.- 2.5-megawatt atmospheric arc jet at Langley Research Center. L-65-144.1

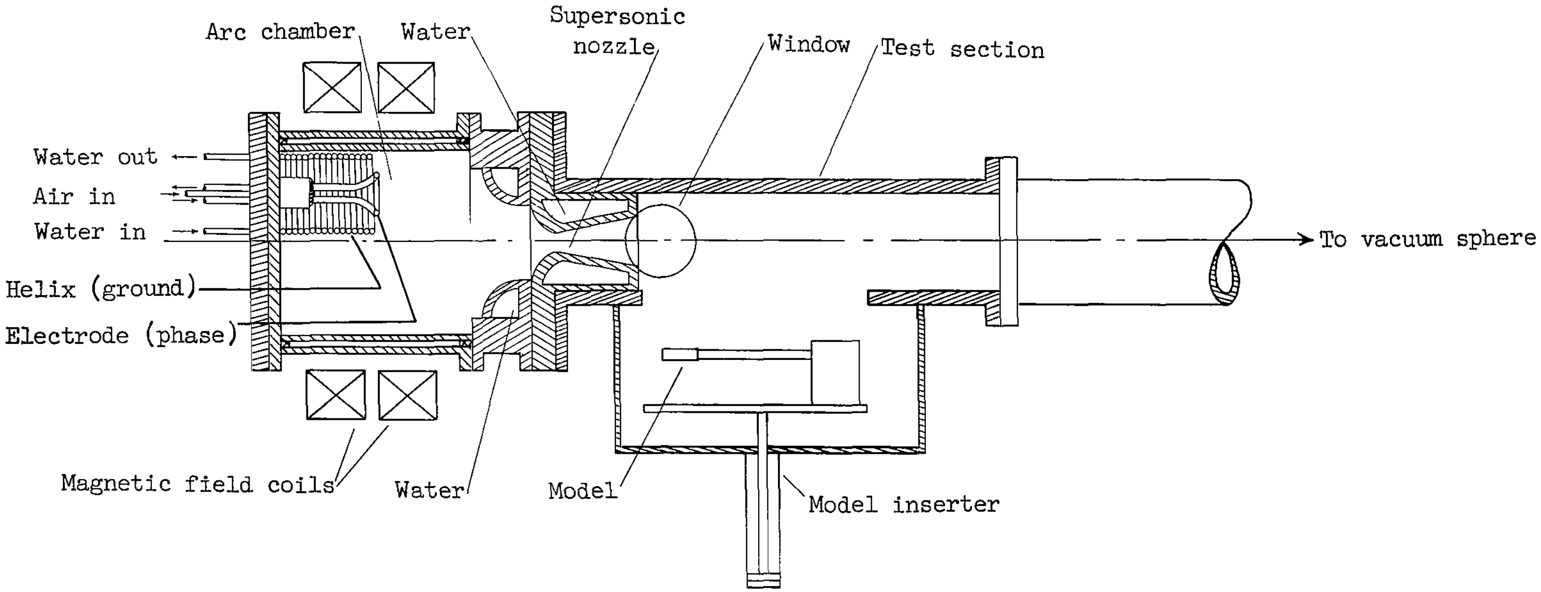

Figure 3.- Diagram of 2.5-megawatt supersonic arc tunnel at Langley Research Center.

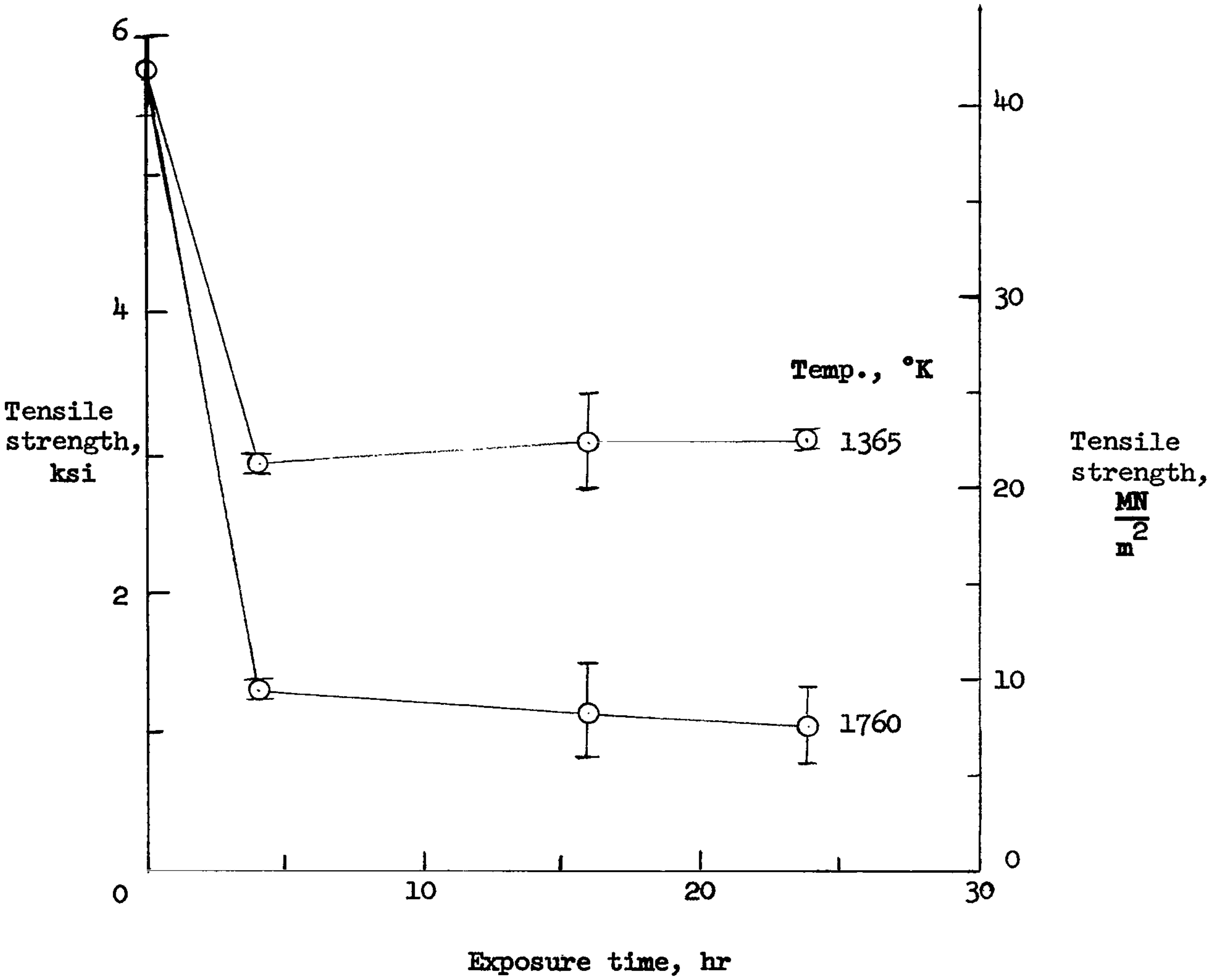

Figure 4.- Tensile strength at room temperature of JTA graphite composite exposed in air at 1365° K and 1760° K. Each point represents an average value for three or four specimens.

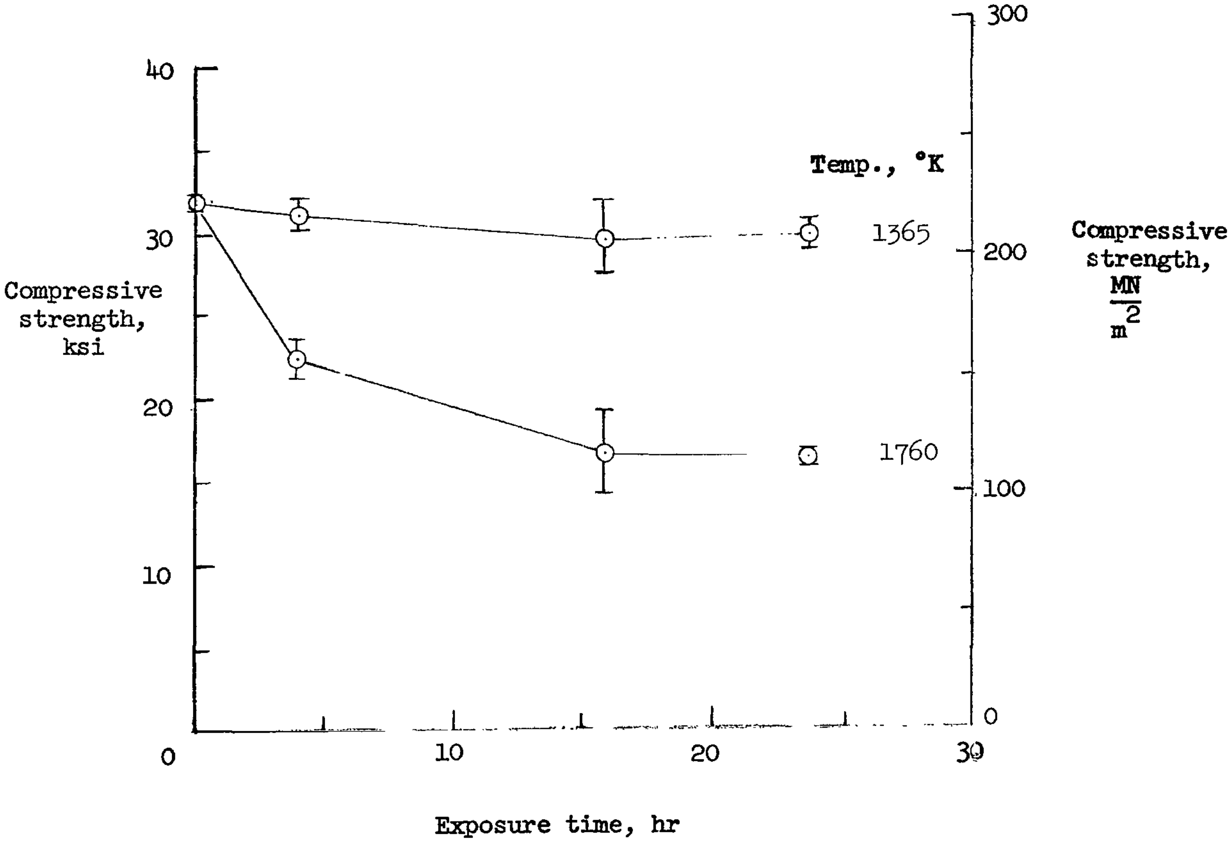

Figure 5.- Compressive strength at room temperature of JTA graphite composite exposed in air at 1365° K and 1760° K. Each point represents an average value for three or four specimens.

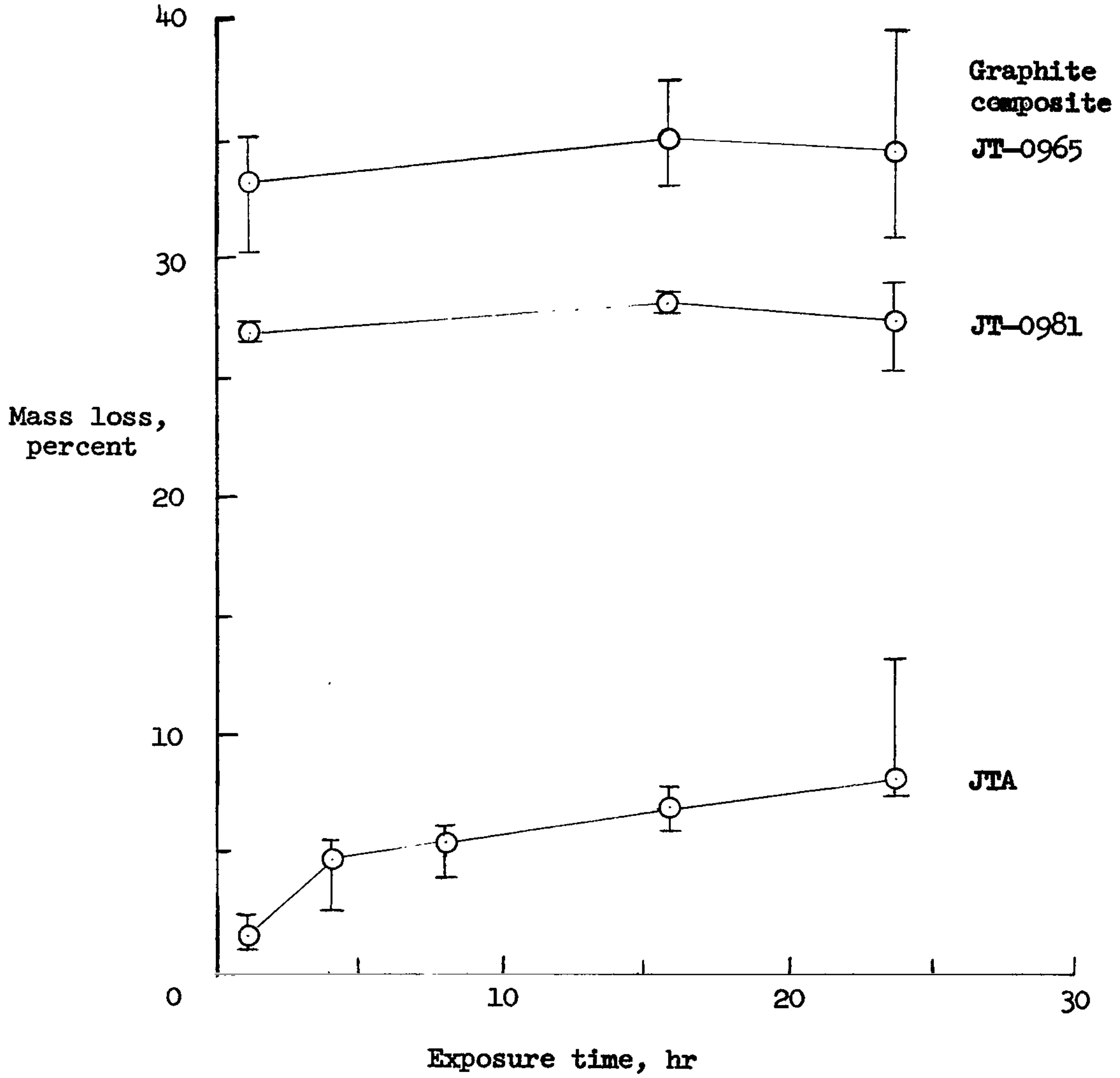

(a) Static oxidation tests at 1365° K.

Figure 6.- Mass loss of JT graphite composites after exposure in air at 1365° K and 1760° K. Each point represents an average value for three or four specimens.

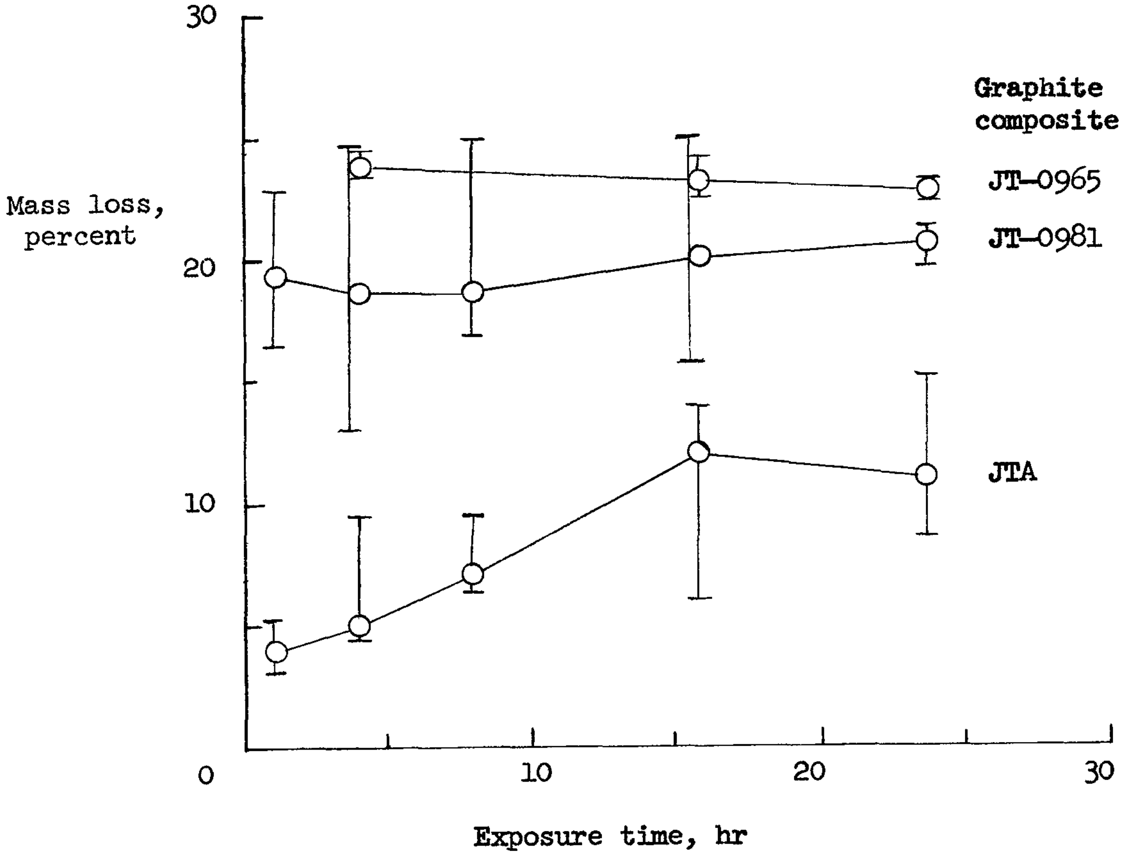

(b) Static oxidation tests at 1760° K.

Figure 6.- Concluded.

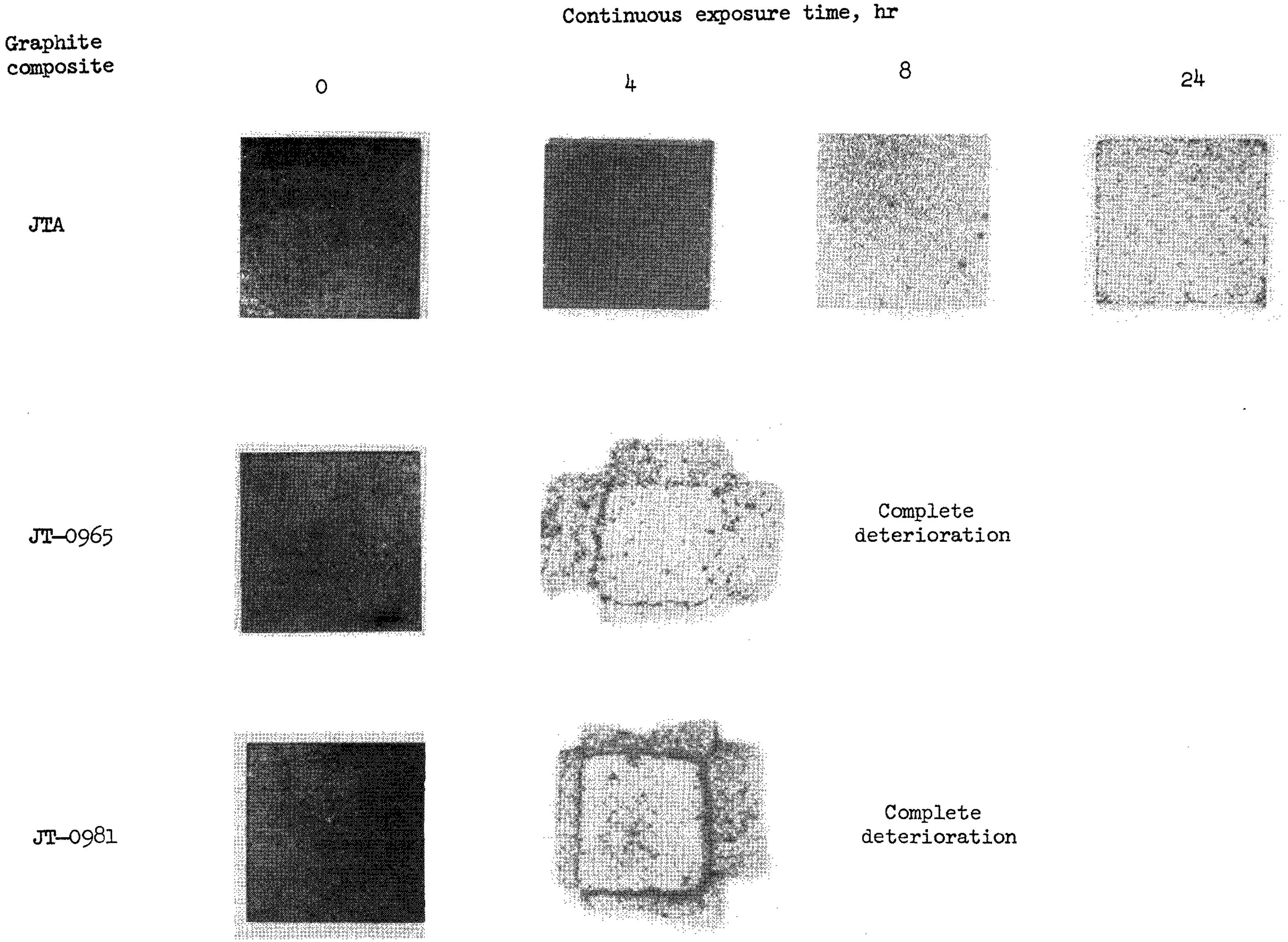

Figure 7.- JT graphite composite oxidation specimens after exposure in static air at 1365^{0} K.

L-67-1088

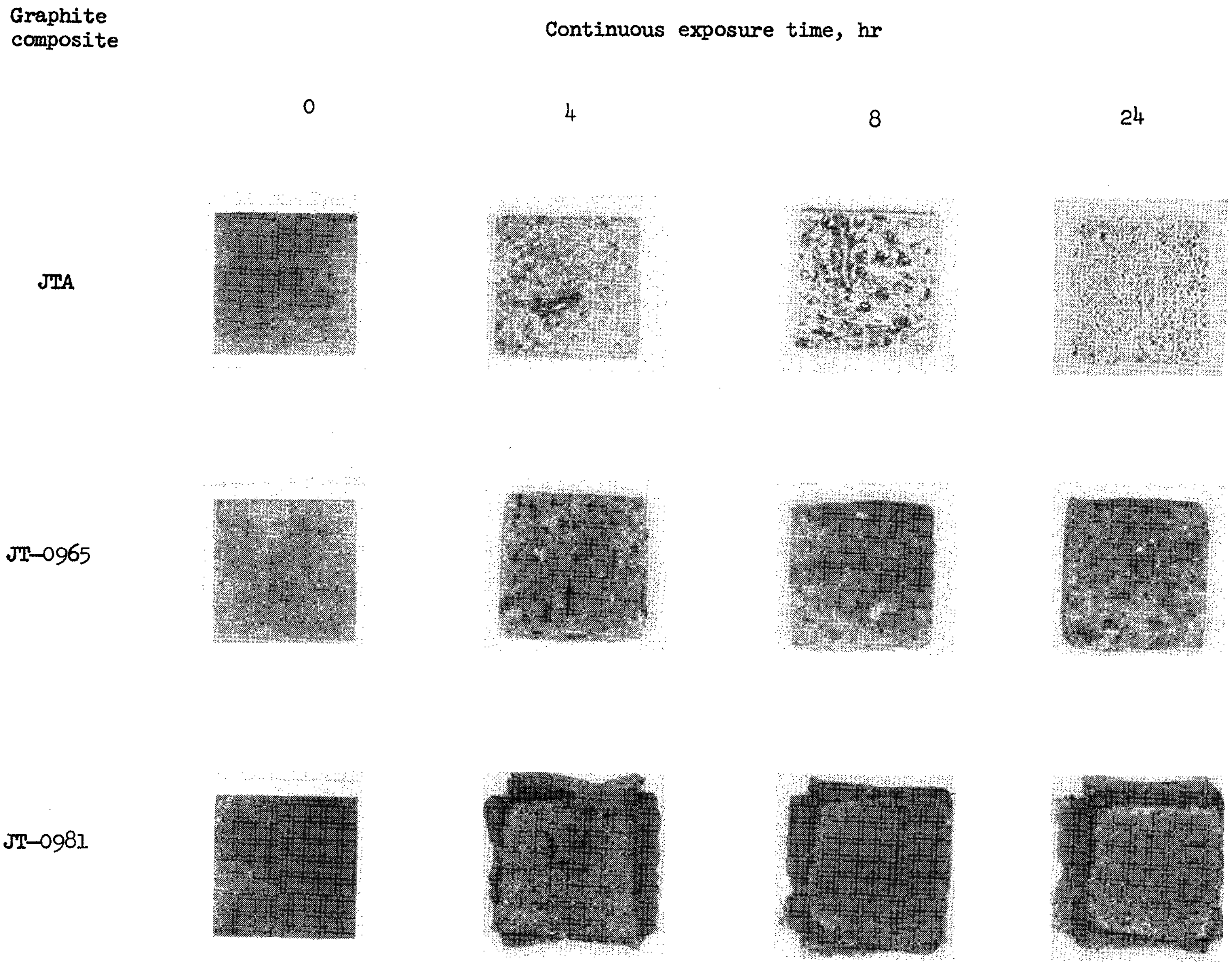

Figure 8.- JT graphite composite oxidation specimens after exposure in static air at 1760° K.

L-67-1089

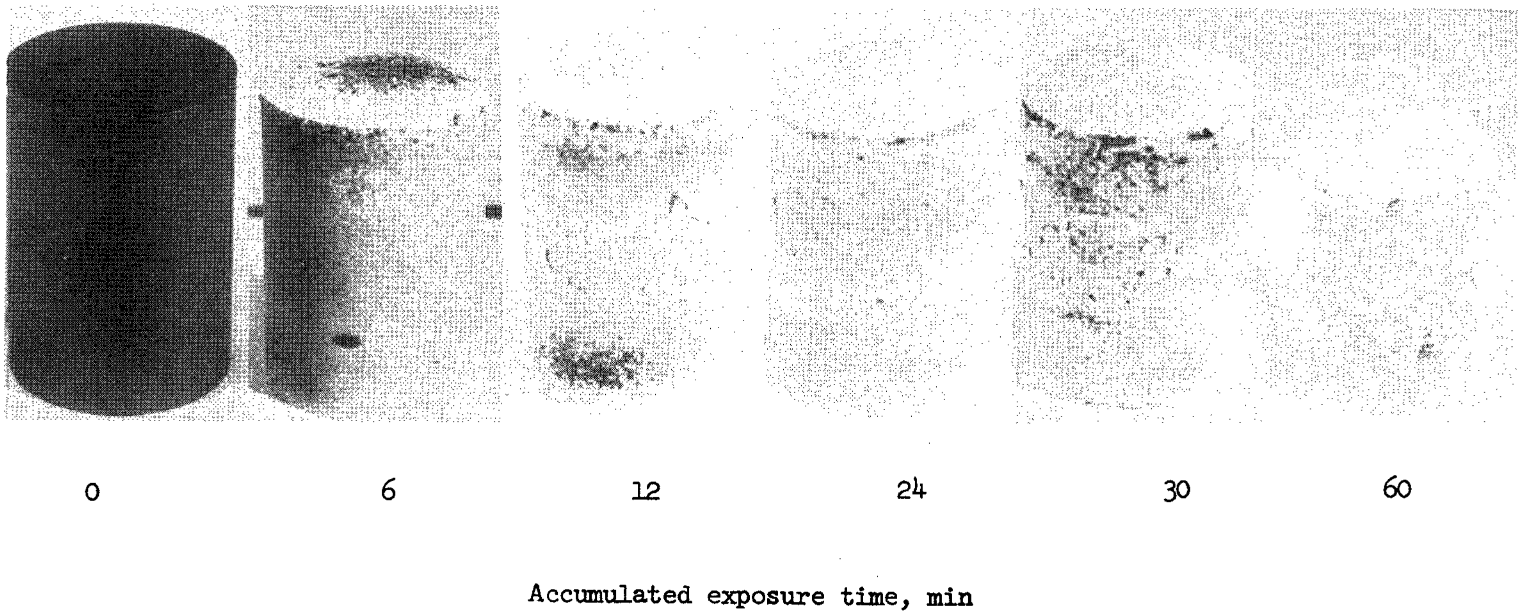

(a) JTA graphite composite.

L-67-1090

Figure 9.- JT graphite composite oxidation specimens subjected to subsonic airflow at surface temperatures of 2475° K.

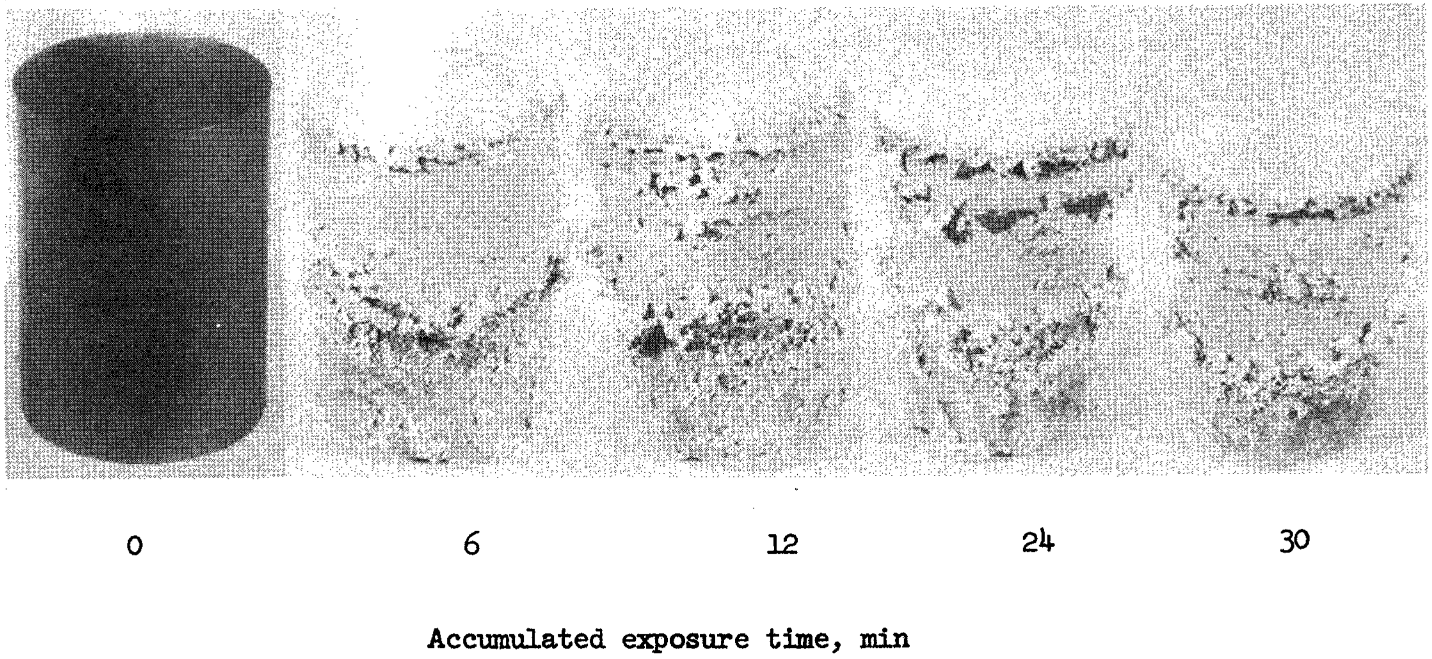

(b) JT-0981 graphite composite.

L-67-1091

Figure 9.- Continued.

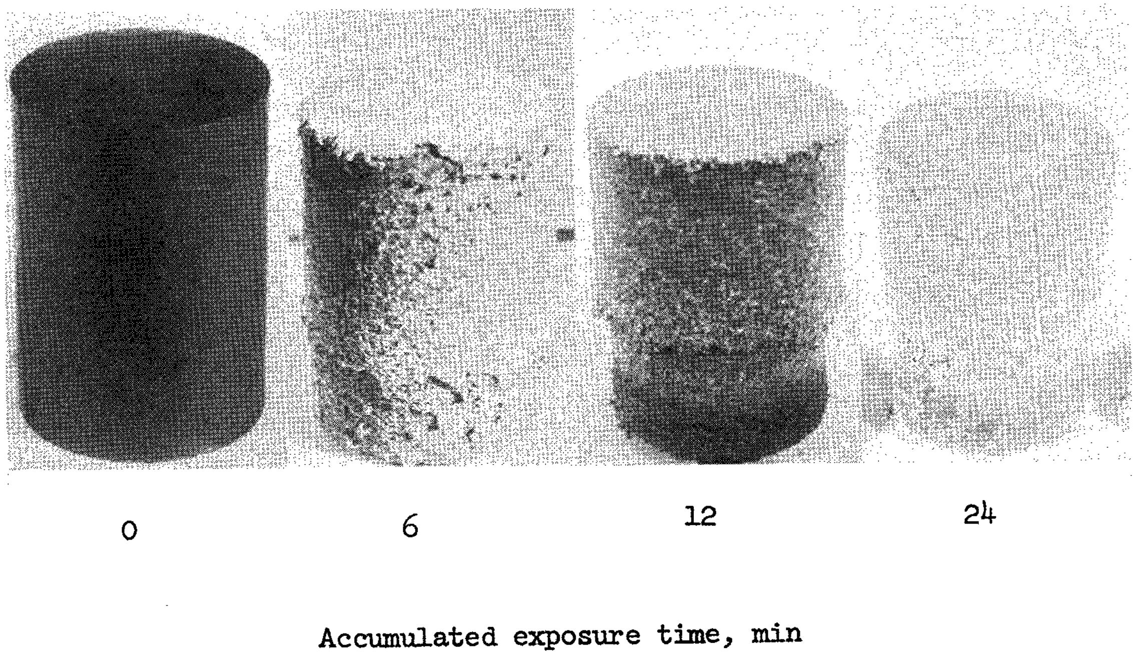

(c) JT-0965 graphite composite.

L-67-1092

Figure 9.- Concluded.

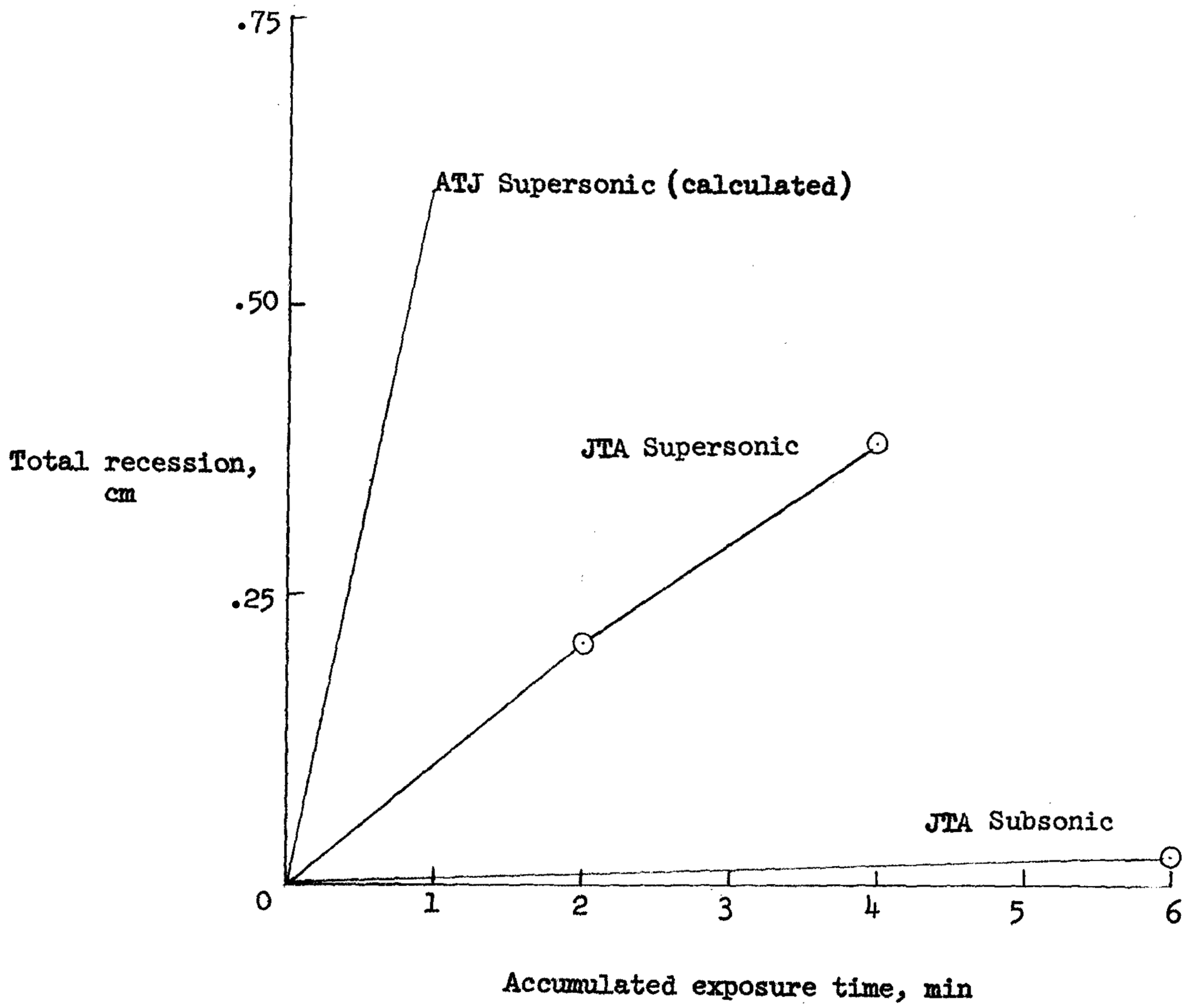

Figure 10.- Surface recession of JTA graphite composite under subsonic and supersonic airflow at surface temperatures of 2475° K and 2500° K, respectively.

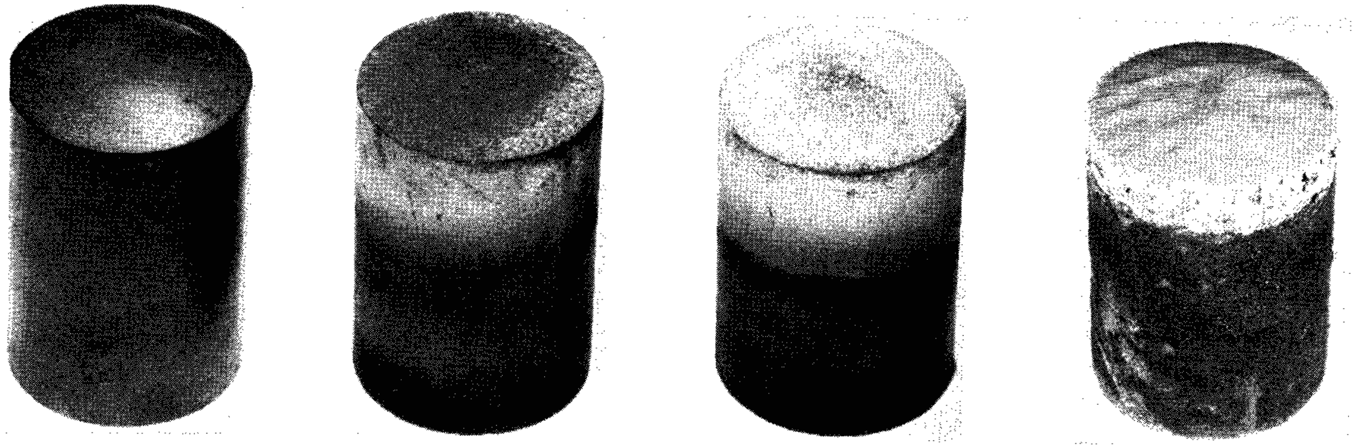

BEFORE TEST

NITROGEN

10 PERCENT O_2
90 PERCENT N_2

AIR

Figure 11.- Dynamic oxidation test specimens of JTA graphite composite subjected to supersonic gas flow for accumulated exposure time of 4 minutes at a specimen surface temperature of 2475° K.

L-67-1093

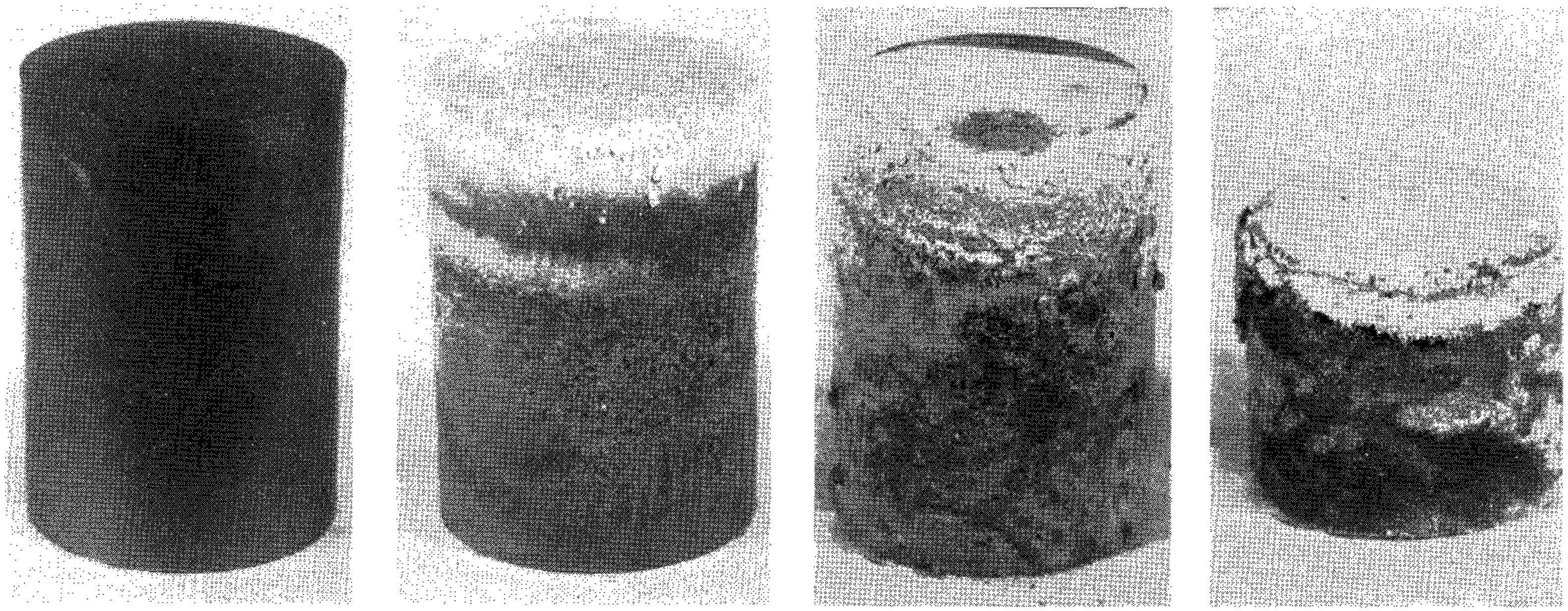

BEFORE TEST

NITROGEN

2755° K

10 PERCENT O_2
90 PERCENT N_2

2865° K

AIR

2975° K

Figure 12.- Dynamic oxidation test specimens of JTA graphite composite subjected to supersonic gas flow for accumulated exposure time of 4 minutes at various specimen surface temperatures.

L-67-1094

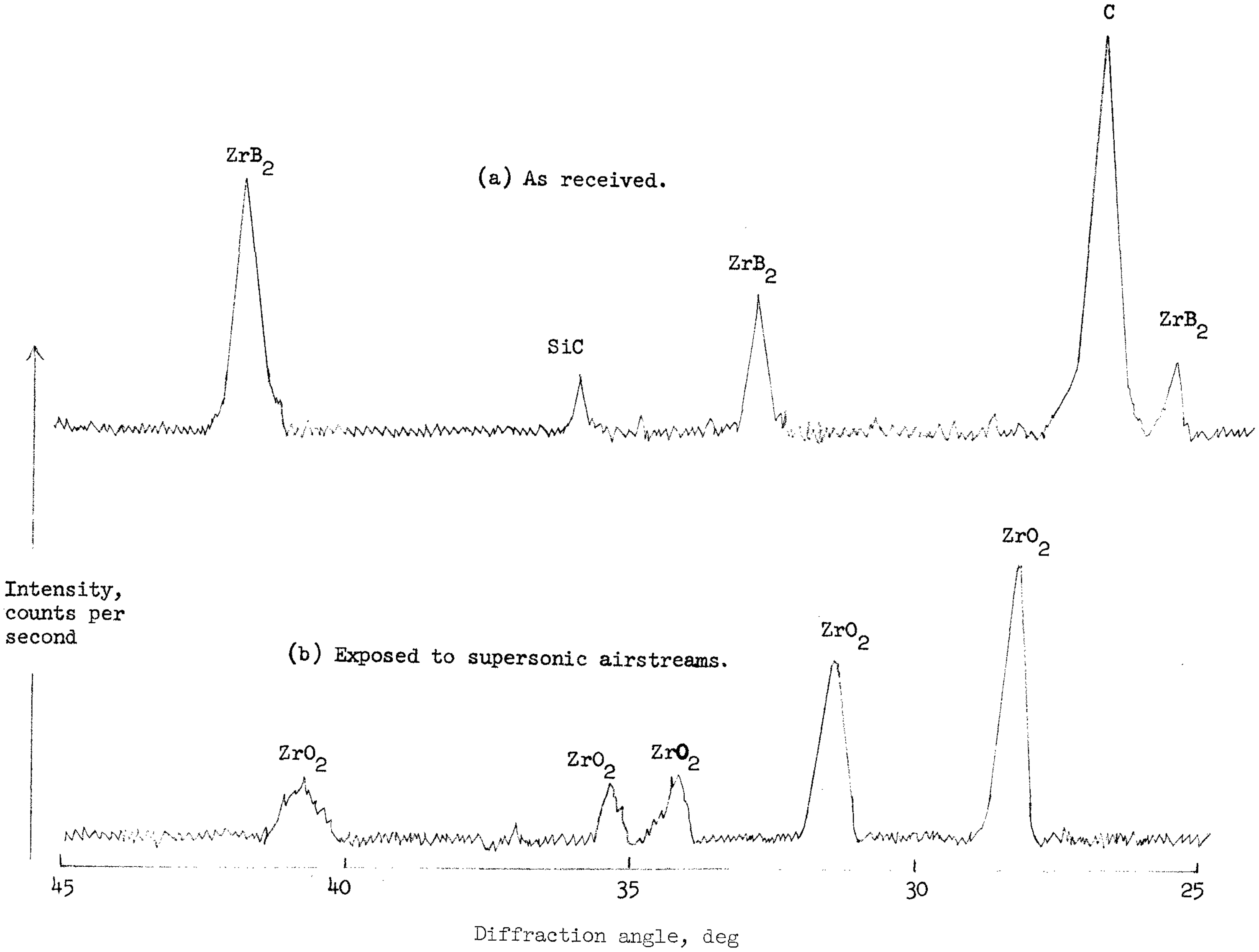

Figure 13.- X-ray diffraction patterns for JTA graphite composite in the as-received condition and after exposure to a supersonic airstream at 2475° K for 2 minutes.

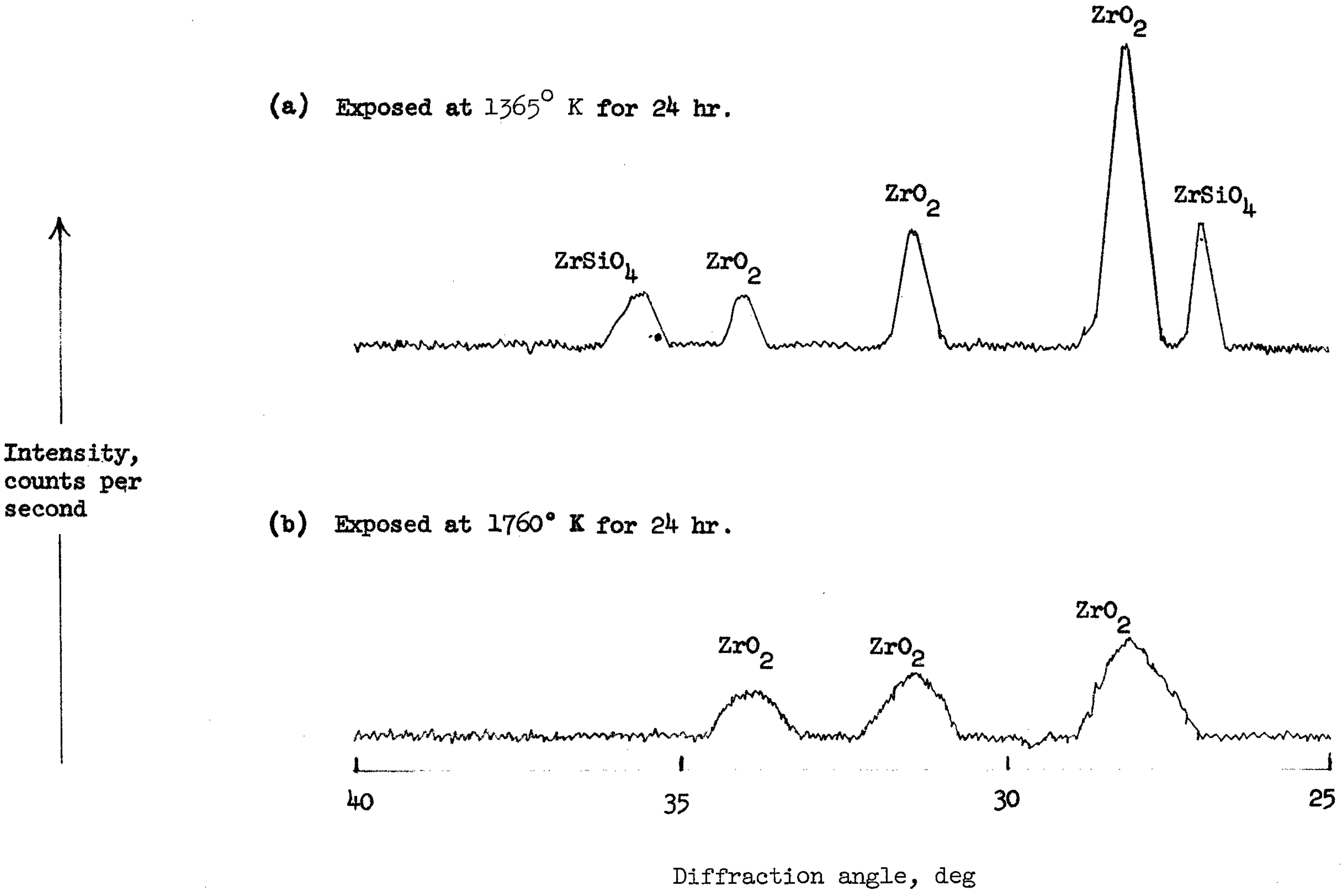

Figure 14.- X-ray diffraction patterns for JTA graphite composite exposed to static air at 1365° K and 1760° K for 24 hours.

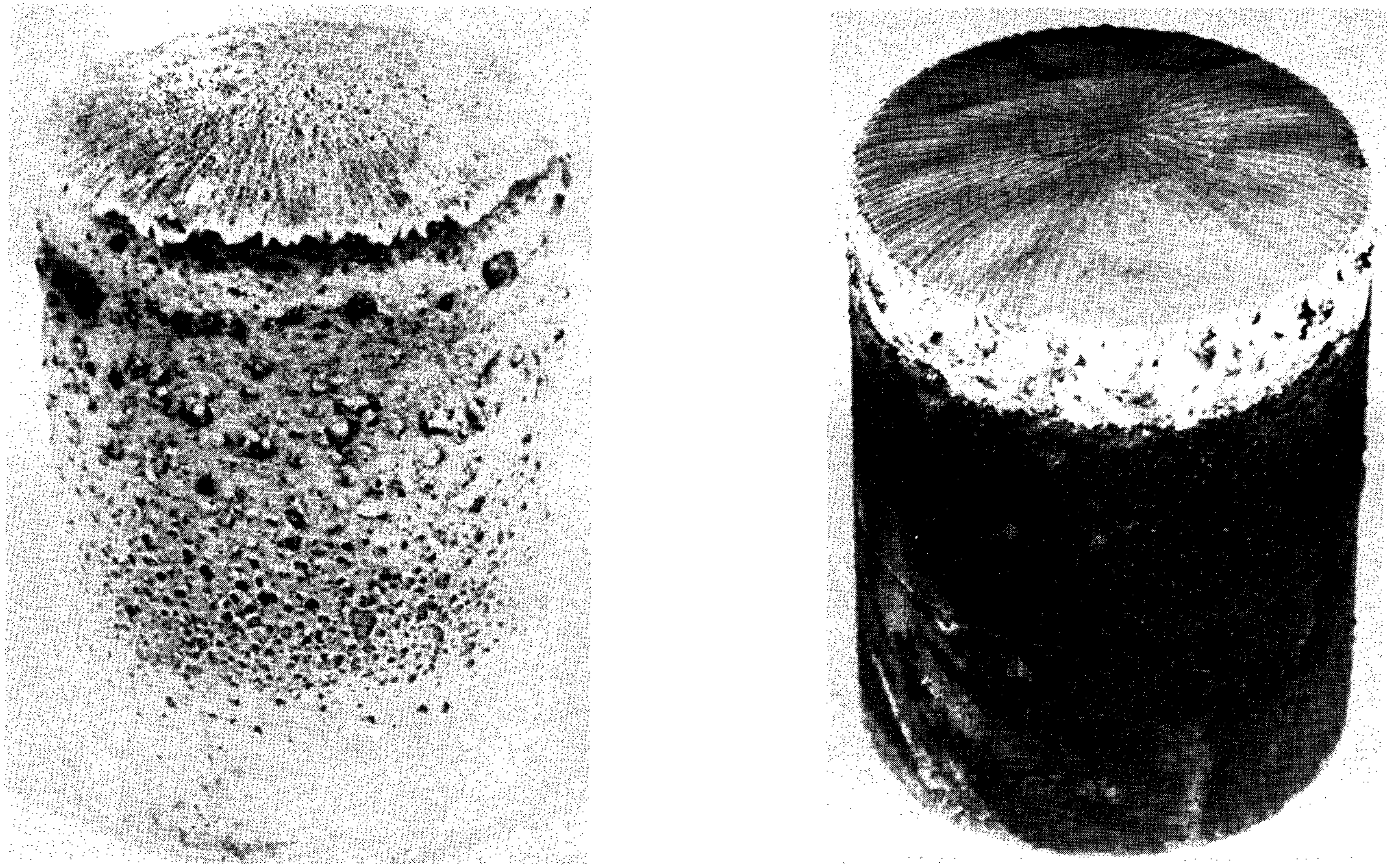

(a) Subsonic airflow; 2475° K; 24 min.

(b) Supersonic airflow; 2500° K; 4 min.

L-67-1095

Figure 15.- JTA coatings formed in subsonic airflow at 2475° K and supersonic airflow at 2500° K. X 2.5.

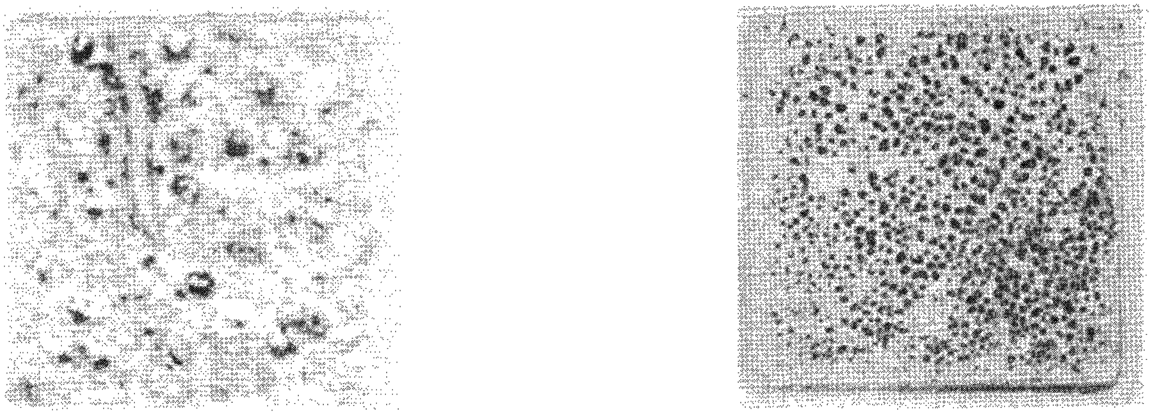

(a) Static oxidation; 1760° K; 8 hr.

(b) Static oxidation; 1760° K; 24 hr.

L-67-1096

Figure 16.- JTA coatings formed in static oxidizing atmospheres at 1760° K after 8 and 24 hours exposure. X 4.

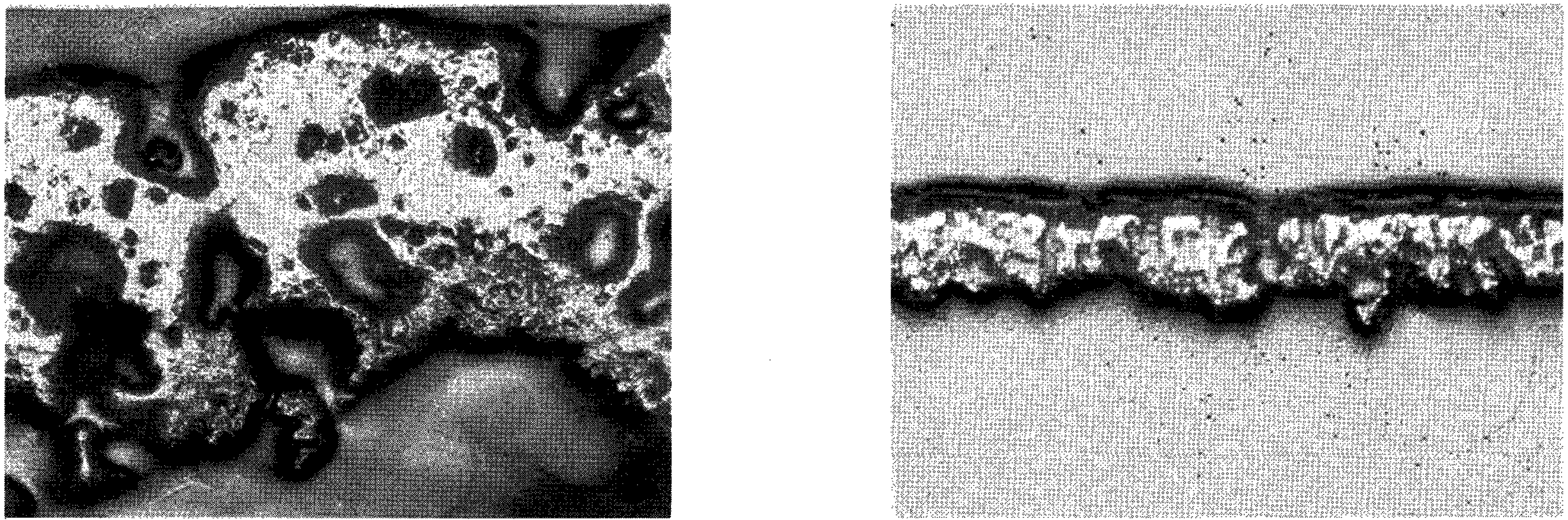

L-67-1097

(a) Subsonic airflow; 2475° K; 6 min; coating thickness, 0.590 mm; X 100.

(b) Supersonic airflow; 2500° K; 4 min; coating thickness, 0.086 mm; X 200.

Figure 17.- Cross sections of JTA coatings formed in subsonic airflow at 2475° K and supersonic airflow at 2500° K.

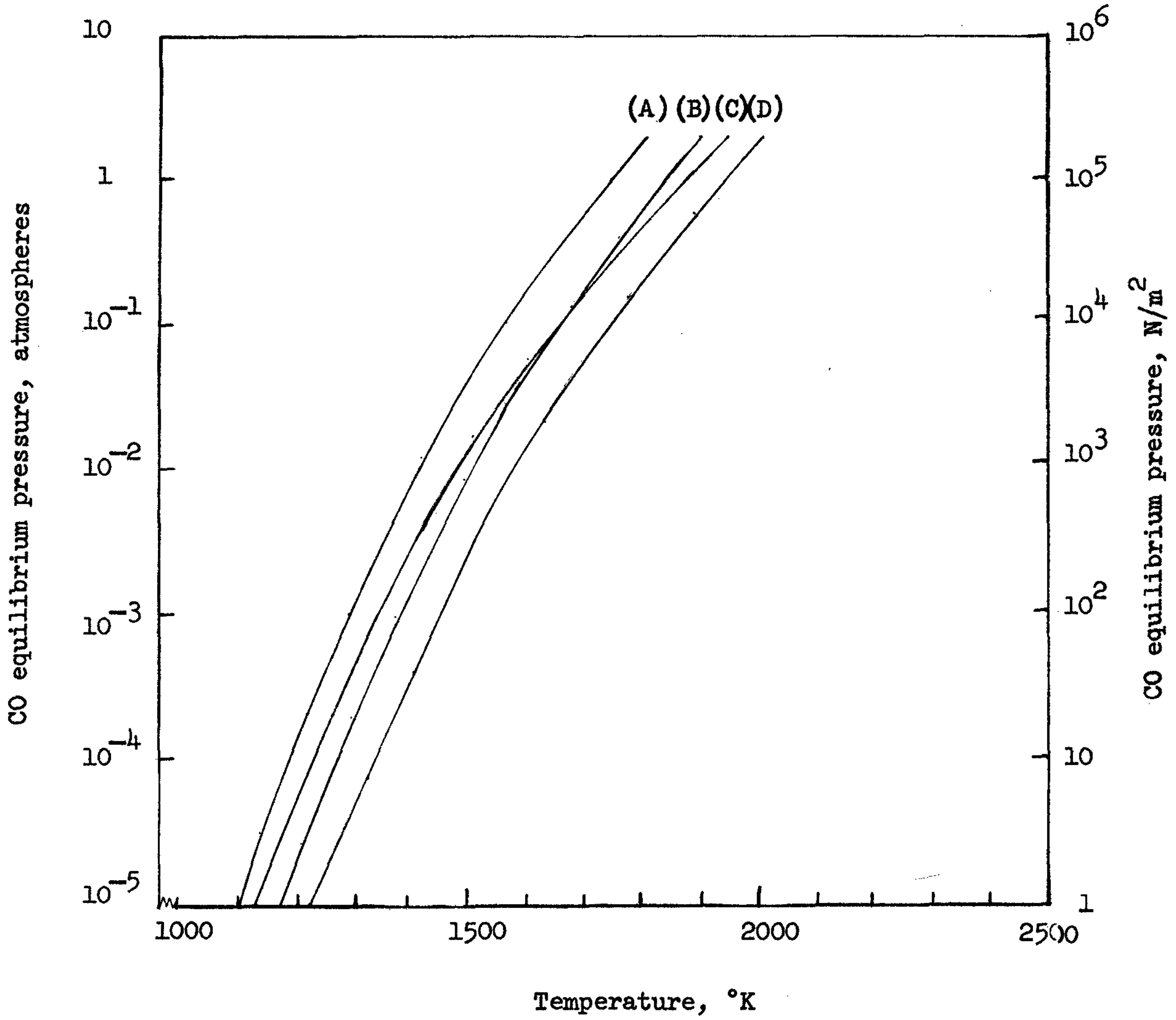

(A) $SiO_2 + 3C \rightarrow SiC + 2CO$

(B) $ZrSiO_4 + 6C \rightarrow ZrC + SiC + 4CO$

(C) $2B_2O_3 + 7C \rightarrow B_4C + 6CO$

(D) $ZrO_2 + 3C \rightarrow ZrC + 2CO$

Figure 18.- Carbon monoxide equilibrium pressures at different temperatures. Reactions between carbon and various refractory oxides (ref. 18) are indicated by equations labeled (A), (B), (C), and (D).

NASA-Langley, 1967 —— 18 L-5287

"The aeronautical and space activities of the United States shall be conducted so as to contribute . . . to the expansion of human knowledge of phenomena in the atmosphere and space. The Administration shall provide for the widest practicable and appropriate dissemination of information concerning its activities and the results thereof."

—NATIONAL AERONAUTICS AND SPACE ACT OF 1958

NASA SCIENTIFIC AND TECHNICAL PUBLICATIONS

TECHNICAL REPORTS: Scientific and technical information considered important, complete, and a lasting contribution to existing knowledge.

TECHNICAL NOTES: Information less broad in scope but nevertheless of importance as a contribution to existing knowledge.

TECHNICAL MEMORANDUMS: Information receiving limited distribution because of preliminary data, security classification, or other reasons.

CONTRACTOR REPORTS: Scientific and technical information generated under a NASA contract or grant and considered an important contribution to existing knowledge.

TECHNICAL TRANSLATIONS: Information published in a foreign language considered to merit NASA distribution in English.

SPECIAL PUBLICATIONS: Information derived from or of value to NASA activities. Publications include conference proceedings, monographs, data compilations, handbooks, sourcebooks, and special bibliographies.

TECHNOLOGY UTILIZATION PUBLICATIONS: Information on technology used by NASA that may be of particular interest in commercial and other non-aerospace applications. Publications include Tech Briefs, Technology Utilization Reports and Notes, and Technology Surveys.

Details on the availability of these publications may be obtained from:

SCIENTIFIC AND TECHNICAL INFORMATION DIVISION
NATIONAL AERONAUTICS AND SPACE ADMINISTRATION
Washington, D.C. 20546